CrossMark

ORIGINAL PAPER

Predicting rock mass deformation modulus by artificial intelligence approach based on dilatometer tests

Mostafa Asadizadeh[1] · **Mohammad Farouq Hossaini**[1]

Abstract Accurately assessing the mechanical behavior of jointed rock mass is one of the most important requirements in the geotechnical and mining engineering projects, including site selection, design, and successful execution. The mechanical behavior of rock mass is significantly affected by the deformation modulus which can be influenced by several parameters. In this paper, a new radial basis function neural network (RBFNN) model was developed to predict deformation modulus based on dilatometer tests at the Bakhtiary dam site, Iran. The model inputs, mostly acquired from geotechnical bore holes, are overburden height (H), rock quality designation (RQD), unconfined compressive strength (UCS), bedding/joint inclination to core axis, joint roughness coefficient (JRC), and filling thickness of joints. High accuracy of prediction was examined by calculating indices such as the variance accounted for, root-mean-square error, mean absolute error, and the coefficient of efficiency. Sensitivity analysis has been conducted on the RBFNN results of Bakhtiary dam site. Based on the obtained results, UCS and RQD are the most effective parameters and inclination of rock joint/ bedding to core axis is the least effective parameter in the deformation modulus of rock mass.

Keywords Rock mass deformability · In situ tests · Bakhtiary dam site · RBFNN

✉ Mostafa Asadizadeh
m.asadizadeh@ut.ac.ir

[1] School of Mining Engineering, College of Engineering, University of Tehran, 1439957131 Tehran, Iran

Introduction

The mechanical behavior of jointed rock masses should be fairly assessed for designing the foundations, slopes, underground openings, and anchoring systems. Rock mass response is governed by intact rock as well as the properties of joints (Hoek 1983). Rock mass is a discontinuous medium with fissures, fractures, joints, bedding planes, and faults. The deformability of rock mass behavior is controlled by the behavior of the mentioned discontinuities or planes of weakness. Reliable characterization of mechanical behavior of jointed\thin bedded rocks is very crucial for safe design of civil structures such as arch dams, bridge piers, and tunnels. The deformability is one of the most important characterizations of rock mass, representing its mechanical behavior. It has been carefully investigated in various rock engineering projects including underground and surface structures (Sridevi and Sitharam 2003). Civil or mining activities in low depth of rock mass occur under low confining pressure. The influence of joints on such cases is completely predominant. In order to investigate the effect of joint pattern of rock mass on its deformability and strength, several researchers have correlated the strength and deformation modulus of the rock mass with several geomechanical indices (Bieniawski 1974, 1979; Serafim and Pereira 1983; Boyd 1993; Hoek 1994; Mitri et al. 1994; Hoek et al. 1995, 2002; Hoek and Brown 1997; Hoek and Diederichs 2006; Verman et al. 1997; Sonmez and Ulusay 1999; Palmström and Singh 2001; Barton 2002; Gokceoglu et al. 2003; Kayabasi et al. 2003; Cai et al. 2004; Zhang and Einstein 2004; Sonmez et al. 2004, 2006). Various methods have been used by the researchers and scientific societies for determining the deformation modulus. These methods are direct measurement through in situ tests, indirect estimations based on rock mass classification methods, laboratory result generalization for rock

Springer

mass, numerical analysis, and soft computing. The conventional methods for determining the deformation modulus are performing in situ tests, for instance dilatometer tests, plate loading tests, flat jack tests, and block tests (Franklin and Dusseault 1989; Yow 1993). As in situ technics can include all obscure in situ parameters of rock mass, they are ranked as the most reliable and comprehensive methods for describing in situ behavior of bedded/jointed rock mass (Goodman 1989; Fahimifar and Soroush 2003). Although the dilatometer test is more preferred for soil, its advantages such as portability and easy to do the test in each depth below the surface have made it appropriate in rock structures as well. The volume of rock affected during dilatometer test is 0.33 m^3 which is much lower than that of plate load test. The numerical simulation of geotechnical problems has been developed rapidly by the advent of high-speed computers. However, not considering all unknown in situ parameters is the most important shortage of numerical methods. The empirical relations (e.g., Bieniawski 1974, 1979; Serafim and Pereira 1983) are well founded enough to predict the properties fairly well. However, they are confined by the degree of non-linearity they can model. Furthermore, statistical relations compel the data along a choosey geometry, which may not always be approbatory, to capture the non-linear relations existed between various parameters.

Soft computing approaches have been found to be very efficacious in the governance non-linear relationships and intelligence prediction of the required parameters. ANN has been one of the most ordinary methods, applied to solve many geotechnical problems, in the last few years (Moosavi et al. 2006, Majdi and Beiki 2010, Ghasemi et al. 2014). Different types of artificial neural networks (ANNs) have been used by the researchers. Radial basis function (RBF) neural network seems to have high potential in presenting non-linear relationships between input and output parameters. This network was basically suggested as a substitution of multilayer perceptron (MLP) neural network for solving complex modeling problems (Luo and Unbehauen, 1999). The architecture of RBF neural network is rather similar comparing to that of MLP neural network. However, the difference between these two neural networks lies in the computational procedure used in input–output alteration. Recently, RBF neural network has been increasingly applied for predicting various geotechnical parameters. For example, it has been used for predicting unconfined compressive strength of soft grounds (Narendra et al. 2006) and elastic modulus of jointed rock mass (Bhushan and Sitharam 2008), fitting creep curve of sandstone (Tan and Zhang 2011), sizing rock fragmentation modeling due to bench blasting (Karami and Afiuni-Zadeh 2012), and identifying instability and risk of underground spaces (Zhouquan et al. 2013; Ding and Zhou 2013). These studies on using

RBF-type neural network in the geotechnical problems also demonstrate its superior generalization capability to capture complex natural non-linear behavior.

So far, RBF neural network has not been used to predict deformation modulus obtained from dilatometer test data. Considering the complexity and highly non-linear behavior of jointed rock mass, RBF neural network seems to be an ideal soft computing tool for predicting the deformation modulus variation in Bakhtiary dam site, Iran. In this research, a new radial basis function neural network (RBFNN) model was developed to predict the deformation modulus based on dilatometer tests at the Bakhtiary dam site. Several parameters have been used to develop the RBFNN model, mostly obtained from geotechnical bore hole log sheets and core samples. These parameters are overburden height (H), rock quality designation (RQD), unconfined compressive strength (UCS), bedding/joint inclination to core axis, joint roughness coefficient (JRC), and filling thickness of joints. Therefore, the objective of this research is to predict deformation modulus based on geotechnical borehole data of jointed rock mass by developing and using RBF neural network.

Basic concept of RBFNN

RBF network is originally a feed forward neural network with a multilayer perceptron. It consists of three layers, input layer, hidden layer (or radial basis layer), and output layer. The network structure is shown in Fig. 1 (Ham and Kostanic 2001). RBFNN is also good at non-linear mapping (Guo et al. 2006; Ham and Kostanic 2001).

The layers are composed of nodes or neurons. The input nodes consist of input variables and hidden nodes of radial basis functions. The nodes of hidden layer are connected to those of output by linear weights, and output nodes produce only the expected number of output variables. The number of input nodes in the input layer and the basis function nodes in the hidden layer are represented in Fig. 1 by $x_1, x_2, \ldots, x_N$ and $\phi_1, \phi_2, \ldots, \phi_M$, respectively. In this figure, w_0 denotes the weight of bias node; $w_1, w_2, \ldots, w_M$ are connection weights between hidden and output nodes; and y is the output corresponding to the input data set. The mapping between input and output for j_{th} hidden node of RBFNN is defined as follows:

$$y(x) = \sum_{j=1}^{M} w_j \phi_j(x) + w_0 \tag{1}$$

where, $y(x)$ is the output corresponding to the multidimensional input vector x, having x_i elements; ϕ_j is the basis function; w_j is the linear weight between hidden and
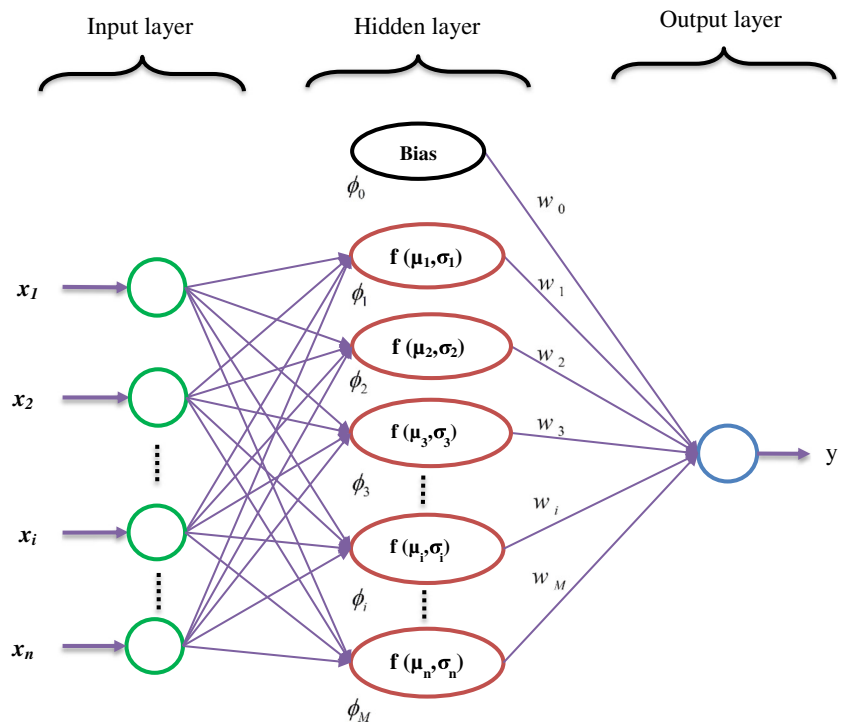
output nodes; M is the number of nodes in the hidden layer; and w_0 is the bias. The bias can participate in the summation as a weight by including an additional basis function ϕ_0 with the value set equal to 1 (Bishop 1995) which then reduces to the form

$$y(x) = \sum_{j=1}^{M} w_j \phi_j(x) \qquad (2)$$

Normalized Gaussian function, the most ordinary function used in the geotechnical engineering, is applied in this study (Narendra et al. 2006; Yilmaz and Kaynar 2011) and defined as

$$\phi_j(x) = \exp\left(-\frac{\|x - \mu_j\|^2}{2\sigma_j^2}\right) \qquad (3)$$

where μ_j and σ_j are the center and width parameters of the basis function ϕ_j, respectively, and $\|.\|$ is the norm of Euclidean distance. Equation (2) in matrix form can be written as follows:

$$y(x) = w\phi \qquad (4)$$

where w is the weight vector. The training of RBFNN is performed by minimizing the error function E. It is the squared difference between network outputs ($y_j(x_i)$) and targets t_{ij} and is presented as

$$E = \frac{1}{2} \sum_{i=1}^{N} \sum_{j=1}^{M} \left[y_j(x_i) - t_{ij} \right]^2 \qquad (5)$$

The training of RBFNN is done in two stages: (1) The center μ and spread σ of the basis function are established from the input data, and (2) the connection weights w are modified to minimize the error function. In this research, the center of hidden neurons was attained by random sampling (Broomhead and Lowe 1988) of input data. Once the center μ for the basis function was established, the spread σ of basis function was computed by normalization method of spread determination. In this method, σ is expressed as twice the average difference between successive centers (Bishop 1995):

$$\sigma_j = 2 \times \sum_{i=1}^{P} \frac{|\mu_{i-1} - \mu_i|}{P} \qquad (6)$$

where μ_{i-1} and μ_i are the successive centers of radial basis functions, and P is the number of RBF centers. Once the center and spread of basis function were established, the network weights were calculated
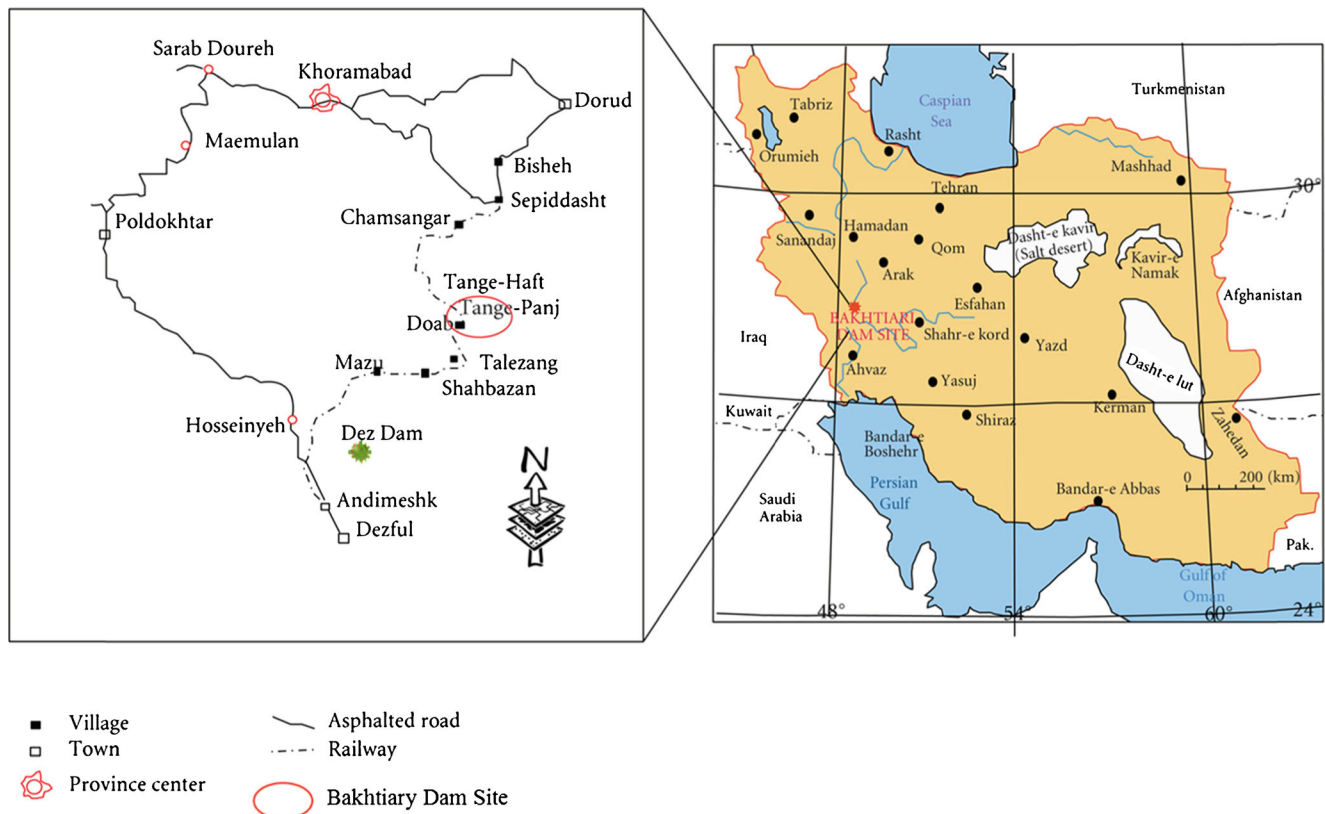
Fig. 2 The location of Bakhtiary Dam and Hydropower Project area on map of Iran and a close view of the dam site on Karun–Dez catchment area map

through pseudo-inverse equation (Bishop 1995) as follows:

$$w^T = \left(\phi^T \phi\right)^{-1} \phi_t^T \tag{7}$$

where

$$w = [w_{ij}]; \quad t = [t_{ij}]; \quad \text{and} \quad \phi = \phi_j(x_i) \tag{8}$$

Case study

Bakhtiary dam site is located in the southwest of Iran, 70 km from the northeast of Andimeshk City (Khuzestan Province) and 65 km from the southwest of Dorud City in Lorestan Province, Iran (Fig. 2). The dam body was designed with maximum height of 325 m and crest length of 509 m at elevation of 840 m asl. It is proposed to construct a dam at this location on the Bakhtiary River in order to provide water for electrical, drinking, and agricultural purposes, increase the volume of regulated water in Dez catchment, decrease the amount of sediment in Dez dam

reservoir, and receive the benefits associated with flood control (BJVC 2009a).

Geological characterization of the Bakhtiary dam site

Bakhtiary dam site and its reservoir are located in the northwestern part of the folded Zagros, at the boundary of Lorestan and Dezful embayment zones. Folded Zagros is a part of Zagros tectono-sedimentary region, confined by thrusted Zagros in the northeast and Khuzestan plain in the southwest. The thick sediments of this zone have been deposited from Triassic to Pliocene era and subsequently folded and deformed during the Plio-Pleistocene by the last Alpine orogenic phase (Motiei 1993). These tectonisms have generated sets of anticlines and synclines which are mostly characterized by vertical axial planes associated with many thrusted faults in Zagros area. Siliceous limestone of Sarvak Formation forms the most important rock of the Bakhtiary dam site and its reservoir. This formation belongs to the Bangestan Group in the Middle Cretaceous Period. Based on the thickness of bedding planes and the existence of siliceous components, this formation is locally divided into seven units, Sv1 to Sv7. The properties of rock units are presented in Table 1.

Table 1 The description of rock units at Bakhtiary dam site (BJVC 2009b)

Rock units	Description
Sv1	Medium to thickly interbedded dark gray marly limestone with black laminated marlstone to shale
Sv2	Thinly to medium bedded dark gray limestone to marly limestone with thin black laminated marlstone to shale interbeds
Sv3	Thinly to medium thick interbedded dark gray marly limestone and siliceous limestone
Sv4	Medium to thickly bedded dark gray limestone with small siliceous nodules
Sv5	Thickly to very thickly bedded dark gray limestone with big siliceous nodules
Sv6	Medium to thickly bedded dark gray limestone and marly limestone with thin interbeds of marlstone
Sv7	Thinly to medium bedded dark gray limestone and marly limestone with thin shale interbeds

Tectonic and structural features of dam site

Several key features of geological structure of the dam site are as follows: folded and duplex structure of Giriveh-Siah Kuh duplex-anticline, fault complex (F1, F2, and F3 fault system), chevron folds and kink band zones, and joint systems. Siah Kuh anticline, and F1 and F3 structures are presented in Fig. 3 (BJVC 2009b).

The evaluation of tectonic history shows that Giriveh-Siah Kuh duplex-anticline and F1–F3 fault system are first-order structures. However, chevron folds are second-order structures, and kink bands and joint sets are the third-order structures. Normal and chevron fold zones are shown in Fig. 4 (BJVC 2009b).

Site investigations

The site has been investigated to provide the geotechnical parameters needed for analyzing the appropriateness of the location and obtaining the required design parameters. The field investigations, conducted in this study, are discontinuities and rock mechanics in situ tests.

Discontinuities

The detailed joint survey includes six exploratory galleries, GR1–GR3 and GL1–GL3 (located on the right bank) and GL1–GL3 (located on the left bank), respectively. Based on these galleries, the rock mass of dam site is intersected by four main discontinuities including limestone beddings in the upstream and downstream, J1A and J1B major joint sets, and J2 and J3 join sets (BJVC 2009a). The geometric properties of discontinuities are presented in Table 2 and Fig. 5.
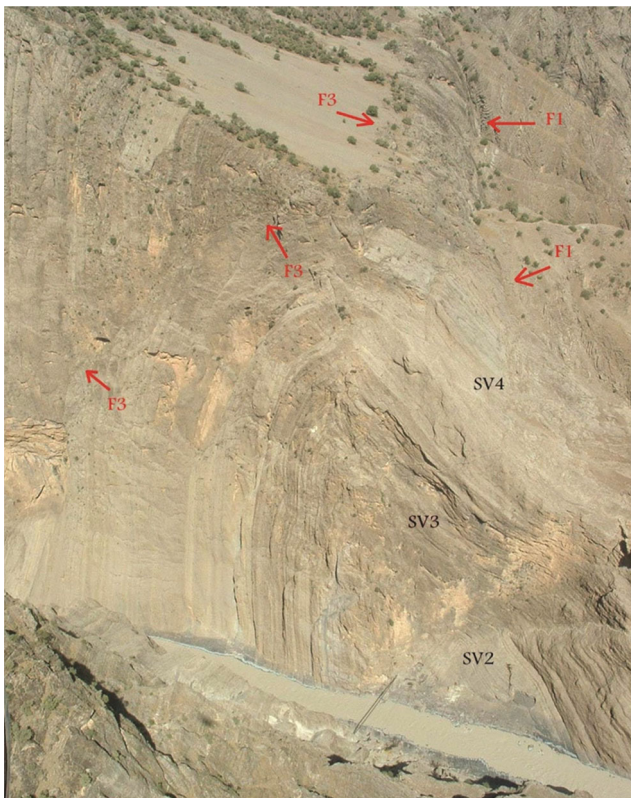

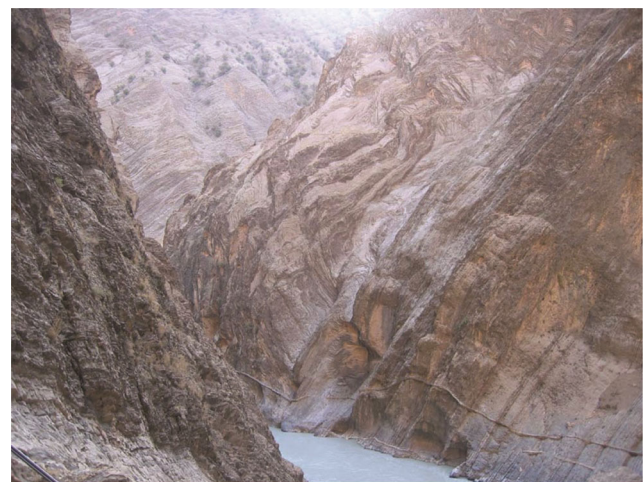**Fig. 3** *Right bank*, Siah Kuh Anticline, and F1 and F3 faults (BJVC 2009b)

Fig. 4 Normal and chevron fold zone of Sv3, *left bank* (BJVC 2009b)

Table 2 Geometric properties of discontinuities (BJVC 2009a)

Type of discontinues	Part	Dip (°)	Dip direction(°)	Spacing (cm)
Bedding	1	75	215	2-600
	2	50	030	0-10
joint set J1	A	70	310	0-10
	B	40	310	0-10
Joint set J2	A	35	125	0-5
	B	75	125	0-5
Joint set J3		15	045	0-5

Rock mechanics in situ tests

The in situ rock mechanics tests have been conducted with the aim of defining the deformation modulus of rock mass, original state of in situ stress, and shear resistance along major discontinuities. From 2004 to 2009, 36 plate load tests (PLTs), 84 dilatometer tests (DLTs), and 9 extra large flat jack tests (FLJTs) were performed at Bakhtiary dam site to determine the characteristics of rock mass deformability. Moreover, the original state of stress was measured by two series of borehole slotter tests and 17 hydraulic fracturing tests. Eighty-six dilatometer tests were carried out in 23 boreholes drilled down in eight exploration galleries (BJVC 2009a). The used dilatometer was IF096 model made up of Interfels with 1-m length and 96-mm diameter, capable of applying up to 10-MPa pressure to the borehole walls. The expansion of borehole diameter is measured by three linear variable differential transformers (LVDTs) built inside the sleeve. The measuring devices are arranged at the angle of 120° relative to each other (Interfels 2002).
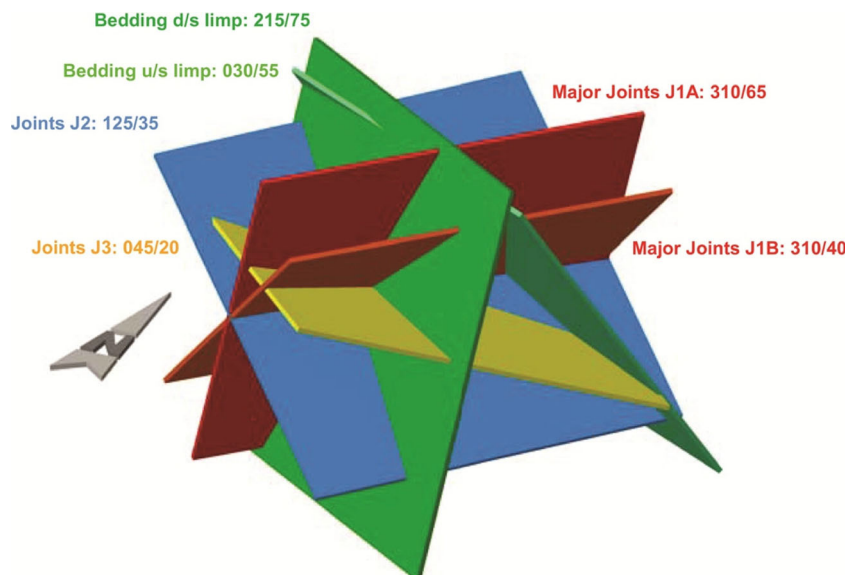

Fig. 6 Overburden (H), rock quality designation (RQD), unconfined compressive strength (UCS), bedding/joint inclination to core axis (I), joint roughness coefficient (JRC), and filling thickness of joints (FT) (BJVC 2009a)

Data sets

Dilatometer test is widely known as a versatile and economical in situ test for measuring the deformation modulus of rock mass. It has been extensively utilized in numerous engineering projects and for measuring rock mass deformation modulus in the boreholes. The main advantages of this test are its affordability, repeatability in several depths of borehole with nearest distance from intact condition, and capability of anisotropy assessment. The data used for training and testing RBFNN model were obtained from a field in situ test program at Bakhtiary dam site. In this study, several parameters have been assessed and collected from core boxes

Fig. 5 Schematic 3D presentation of discontinuities in the project area (BJVC 2009a)

(Fig. 6). These parameters are overburden height (H), rock quality designation (RQD), unconfined compressive strength (UCS), bedding/joint inclination to core axis (I), joint roughness coefficient (JRC), and filling thickness of joints (FT). Moreover, geotechnical investigations have been conducted according to International Society for Rock Mechanics

(ISRM) suggested method (Barton 1978) to develop a RBFNN model for predicting rock mass deformation modulus at Bakhtiary dam site.

All data have been statistically analyzed carefully, and the histograms of input and output data are presented in Figs. 7 and 8, respectively.
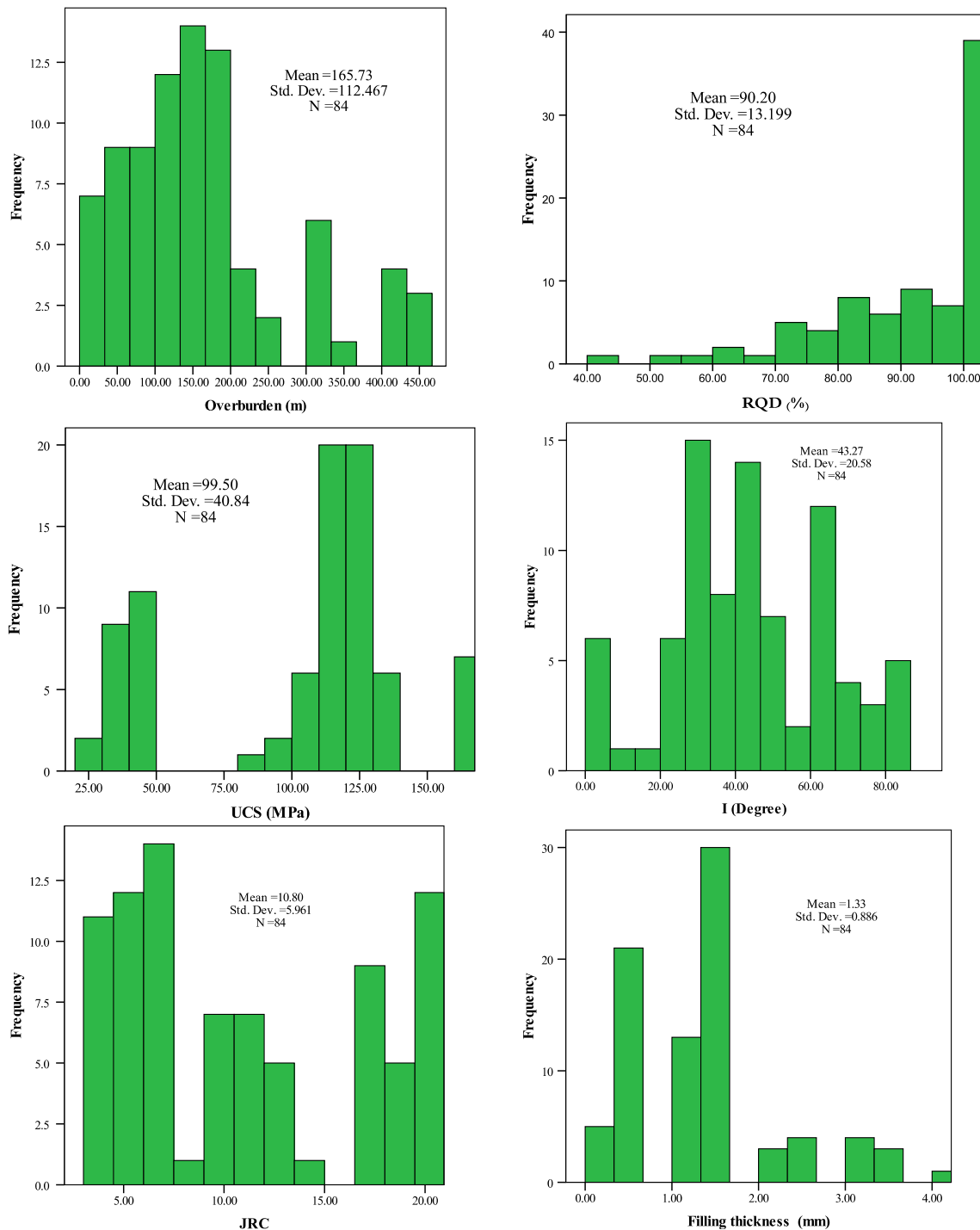

Fig. 7 The histogram of input parameters including: overburden (H), rock quality designation (RQD), unconfined compressive strength (UCS), bedding/joint inclination to core axis (I), joint roughness coefficient (JRC), and filling thickness of joints (FT) (BJVC 2009a)
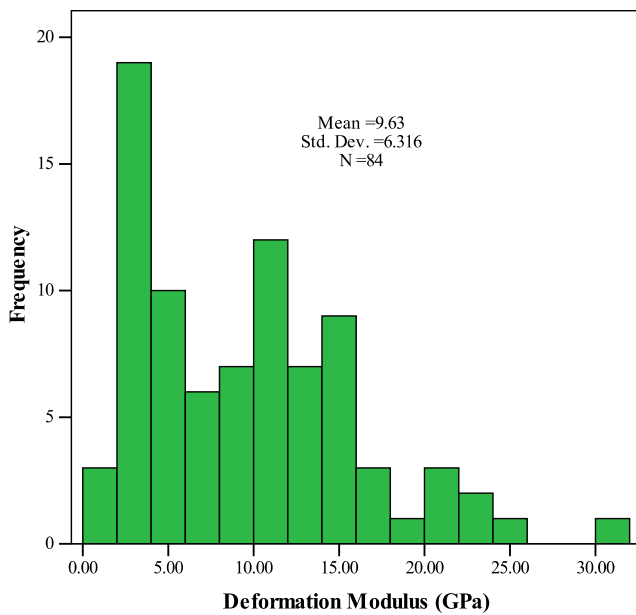
Fig. 8 The histogram of deformation modulus (BJVC 2009a)

Calculation procedure of deformation modulus

In general, dilatometer tests were performed according to ISRM suggested method for deformability determination using a flexible dilatometer with radial displacement measurements (Ladanyi 1987). Figure 9 shows a typical pressure–displacement curve along with graphical definitions of peak-to-peak modulus of deformation D_{PP} as well as modulus of elasticity E. Based on this figure, D_{PP} reflects both elastic and inelastic behavior of the tested rock mass between the first and third cycle. Accordingly, E represents elastic properties of the

rock mass during loading of the third cycle in the stress range between setup pressure and maximum pressure of the second cycle (6 MPa).

The values of moduli have been calculated based on the formulas proposed by Ladanyi (1987). Equation (8) is the standard formula for calculating moduli values using flexible dilatometer with radial displacement measuring system in competent and/or widely jointed rock masses:

$$E_d = (1 + \nu_R)D \frac{\Delta p_i}{\Delta D} \qquad (9)$$

where E_d is the modulus of deformation (MPa), ν_R is the Poisson's ratio of rock mass (taken as 0.3), D is diameter of borehole (mm), Δp_i is the pressure increment within the considered segment (MPa), and ΔD is the corresponding average change in drill hole diameter (D, mm).

Equation (9) has been developed in 1980s for calculating above mentioned parameters in closely jointed rock masses when the applied pressure exceeds about twice the average ground pressure around the drill holes, and is defined as follows:

$$E_d = D \frac{P_i}{\Delta D}(1 + \nu_R)\left[(1-\nu_R)\ln\left(\frac{p_i}{2p_0}\right) + 1\right] \qquad (10)$$

where P_i is the applied pressure (MPa), and p_0 is the average ground pressure (MPa).

Poisson's ratio of rock mass has been measured from petite seismic tests in exploratory galleries. The average ground pressure was obtained through hydraulic fracturing tests. Table 3 presents the general estimations of horizontal principal stresses in the vicinity of the dam site.

Fig. 9 Typical pressure–displacement curve, peak-to-peak modulus of deformation (Dpp) and modulus of elasticity (E) of rock mass in a dilatometer test (BJVC 2009a)
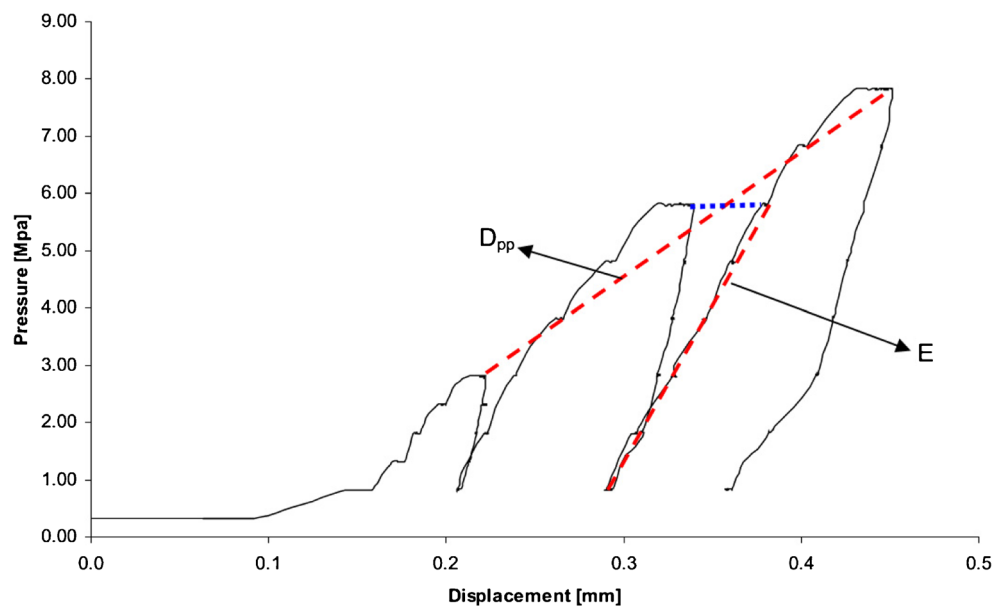
Table 3 In situ stress measured by hydraulic fracturing test at Bakhtiary dam site (BJVC 2009a)

Minimum horizontal stress (MPa)	Maximum horizontal stress (MPa)	The orientation of maximum horizontal stress (degree)
1.62±0.91	2.70±1.34	N57±36°

Applying RBFNN to predict rock mass deformation modulus

The main steps to develop RBFNN model are selecting input data, raw data normalization process, number of input and hidden neurons, and the distribution of RBF function. These stages are described briefly in the following.

Partitioning of input data

It is necessary to select an appropriate division of input data for training and testing of the network. In the present research, 84 data sets were prepared for RBFNN modeling, about 76 % of which for developing and the rest for testing the model. Sorting method was utilized in selecting testing data sets. The parameters and data sets applied in the modeling are shown in Tables 4 and 5, respectively.

Raw data normalization process

Normalization of data concerns about fast processing and convergence during training and minimizing the prediction error (Rojas 1996). The data are prepared by different methods such as cleaning, integration, transformation, and reduction. The main purpose is to guarantee their qualities prior to entering any learning algorithm.

One of the of data preparation methods is data transformation methods, especially normalization. Data normalization is a fundamental preprocessing step for

mining and learning from data. In this research, all input and output data were normalized using Eq. (10):

$$Z = \frac{X-\mu}{\sigma} \tag{11}$$

where Z is the normalized data, X is the raw data, μ is the mean, and σ is the standard deviation.

Input variables, and number of input and hidden neurons

The architecture of RBFNN is determined by choosing the number of neurons in the input layer. On the other hand, in a RBF model, choosing the input variables governs the number of neurons in the input layer. Therefore, selecting the appropriate type and number of input variables is an important factor in a RBFNN model for obtaining satisfactory prediction results. The data enter the network through input layer. The number of input layer completely depends on the problem. In this study, the parameters overburden height (H), rock quality designation (RQD), unconfined compressive strength (UCS), bedding/joint inclination to core axis (I), joint roughness coefficient (JRC), and filling thickness of joints (FT) have been considered for the deformation modulus and are presented in Fig. 10.

The number of neurons in the hidden layer was determined using self-learning method, a default learning procedure in Matlab neural network toolbox (nntool). This is an automatic method for obtaining the optimum number of hidden neurons. Determining the maximum number of hidden neuron is predefined in the self-learning method of network architecture. Accordingly, the training is started with a single neuron in the hidden layer. In training phase, while the desired network error minimization is not achieved, new neurons are added successively to the hidden layer and new connection weights are generated. Then, immediately, the training phase is repeated allowing the new connection weights to acquire the portion of knowledge base not stored in the old connection weights. The above steps are repeated and new hidden nodes are added

Table 4 Input and output parameters used in RBFNN model (BJVC 2009a)

Type of data	Parameter	Unit	Symbol	Minimum	Maximum
Input	Overburden height	m	H	6	459.4
	Rock quality designation	%	RQD	42	100
	Unconfined compressive strength	MPa	UCS	24	160
	Bedding/joint inclination to core axis	Degrees	I	2.5	85
	Joint roughness coefficient	–	JRC	3	20
	Filling thickness	mm	FT	0	4
Output	Deformation modulus	GPa	M	1.49	30.6

Table 5 The data used in learning phase of RBFNN model (BJVC 2009a)

No	H (m)	RQD (%)	UCS (MPa)	I (degrees)	JRC	FT (mm)	M (Gpa)
1	20.40	93.00	125.00	52.00	4.00	1.50	30.60
2	45.50	100.00	69.00	75.00	5.00	1.50	3.47
3	169.25	100.00	106.50	20.00	7.00	1.50	11.90
4	431.90	100.00	94.00	45.00	7.00	0.50	15.38
5	138.60	80.00	94.00	85.00	19.00	0.50	2.35
6	174.30	73.00	25.00	55.00	17.00	3.00	3.73
7	459.40	100.00	87.50	40.00	9.00	0.50	22.38
8	192.25	100.00	106.50	80.00	11.50	1.00	20.30
9	174.30	42.00	96.50	42.00	13.00	1.00	2.02
10	121.50	57.00	19.00	36.25	10.50	1.00	13.47

H overburden height, *RQD* rock quality designation, *UCS* unconfined compressive strength, *I* bedding/joint inclination to core axis, *JRC* joint roughness coefficient, *FT* filling thickness, *M* deformation modulus

successively, needed for the highest network error reduction. The appropriate network architecture is automatically determined in such process. In the self-learning method of network architecture determination, the spread σ of input data was not estimated using Eq. (6) during training. However, the spread σ of network is manipulated to find its value at which the least error occurs in the network.

The neural network structure after learning

Radial basis function (RBF) network typically has three layers: an input layer, a hidden layer with a non-linear RBF activation function, and a linear output layer. Radial basis networks can be used to approximate functions. RBF adds neurons to the hidden layer of a radial basis network until it meets the specified mean squared error goal. The spread σ of RBF was pre-established by random sampling of input data through trial and error method of establishing the number of hidden neurons (Broomhead and Lowe 1988); therefore, it remained constant. The characteristic of hidden layer is presented as follows:

Goal: Mean squared error goal (default = 0.0)
Spread: Spread of radial basis functions (σ = 1.28)
MN: Maximum number of neurons in hidden layer (MN = 60)
DF: Number of neurons added between displays (DF = 4)

Prediction performance

In order to evaluate the prediction performances, model extraction has been performed for ARBFNN model by data testing of database. Data testing includes about 20 data sets, randomly selected from database and not used in the model development. Ten samples of testing data are presented in Table 6.

Performance index

The performance of RBF neural network was evaluated using variance accounted for (VAF), root-mean-square error (RMSE), mean absolute error (MAE), and the coefficient of efficiency (CE), defined as follows:

$$VAF = 100 \left(1 - \frac{\mathrm{var}\left(u_k - \hat{u}_k\right)}{\mathrm{var}(u_k)} \right) \tag{12}$$

$$RMSE = \sqrt{\frac{1}{N} \sum_{i=1}^{n} \left(\hat{u}_k - u_k\right)^2} \tag{13}$$

$$MAE = \frac{1}{N} \sum_{k=1}^{N} \left|\hat{u}_k - u_k\right| \tag{14}$$

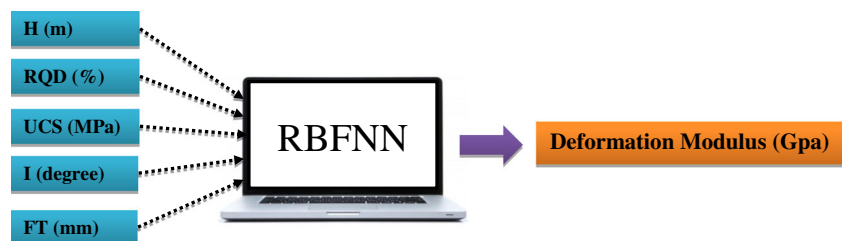**Fig. 10** Architecture of RBFNN model for predicting deformation modulus

Table 6 Sample of data used in testing phase of RBFNN model (BJVC 2009a)

No	H (m)	RQD (%)	UCS (MPa)	I (degrees)	JRC	FT (mm)	M (GPa)
1	330.30	100.00	120.00	35.00	20.00	2.50	11.37
2	108.65	88.00	112.00	35.00	3.00	1.50	7.42
3	439.20	88.00	120.00	50.00	7.00	0.50	10.16
4	33.00	75.00	112.00	15.00	11.00	0.50	6.09
5	24.60	95.00	160.00	30.00	7.00	1.50	22.46
6	166.00	100.00	32.00	65.00	5.00	0.00	4.61
7	49.70	100.00	112.00	70.00	20.00	2.50	6.92
8	144.30	100.00	40.00	45.00	13.00	0.50	3.10
9	148.00	87.00	40.00	52.50	5.00	0.50	10.31
10	124.60	66.00	40.00	32.50	18.00	1.50	3.15

H overburden height, *RQD* rock quality designation, *UCS* unconfined compressive strength, *I* bedding/joint inclination to core axis, *JRC* joint roughness coefficient, *FT* filling thickness, *M* deformation modulus

$$CE = 1 - \frac{\sum_{k=1}^{N}\left(\hat{u}_k - u_k\right)^2}{\sum_{k=1}^{N}\left(\hat{u}_k - \overline{\hat{u}}\right)^2} \qquad (15)$$

where *var* is the variance; $\hat{u}_k$ and u_k are the *k*th predicted and observed values of target, respectively; $\overline{\hat{u}}$ is the mean of predicted target values; and *N* is the number of observations for which the error has been computed. VAF index displays the degree of difference between the variances of measured and predicted data sets. The values of VAF closer to 100 % indicate low variability and consequently better prediction capabilities. RMSE index is the measure of bias between measured and predicted data. The lower the RMSE, the better the model performs (Habibagahi and Katebi 1996; Den Hartog et al. 1997). Ideally, the value of RMSE and MAE should be zero and that of CE should be one. The suggested model has been validated using threefold cross-validation method. The relevant outputs were controlled with performance indices. For the purpose of cross-validation, 84 data were divided into two sets of 64 and 20 for training and testing data, respectively. The process was applied in three different arrangements. Testing data were completely different in each arrangement. The results obtained from applying three data sets to the models are presented in Table 7. Cross-validation indicated that the models worked very well with different input data. Therefore, overfitting cannot be a problem and the models could be comprehensive.

Modeling results

Figure 11 presents the average results obtained from simulating RBFNN models. Figure 12 shows measured and predicted

deformation modulus of these models for 20 series of testing data. According to these figures, the average coefficient of correlation (R^2) of RBFNN model is 0.89. This high coefficient of correlation shows the accordance between the results of RBFNN model and measured data.

Sensitivity analysis

Sensitivity analysis was performed on the model outputs using cosine amplitude method (CAM) (Grima 2000; Jang et al. 1997; Ross 1995) to determine the most effective input parameters in the average output parameter. In this method, the data pairs are expressed in a common X-space and used to construct a data array *X* which is defined as

$$X = \{X_1, X_2, X_3, \dots X_m\} \qquad (16)$$

Each element (X_i) in the data array *X* is a vector of lengths and expressed as follows

$$X_i = \{x_{i1}, x_{i2}, x_{i3}, \dots, x_{im}\}_1 \qquad (17)$$

Thus, each data pair can be considered as a point in *m*-dimensional space, where each point requires *m*-

Table 7 Average model performance indices (BJVC 2009a)

Data sets	Testing data	R^2	VAF (%)	RMSE	MAE	CE
1	20	0.89	83.77	2.57	2.14	0.88
2	20	0.91	84.67	2.49	2.03	0.88
3	20	0.88	82.03	2.72	2.34	0.87
Average	20	0.89	83.49	2.59	2.17	0.88

R^2 coefficient of correlation, *VAF* variance accounted for, *RMSE* root-mean-square error, *MAE* mean absolute error, *CE* coefficient of efficiency

Fig. 11 Comparing the measured and average predicted values of deformation modulus (BJVC 2009a)
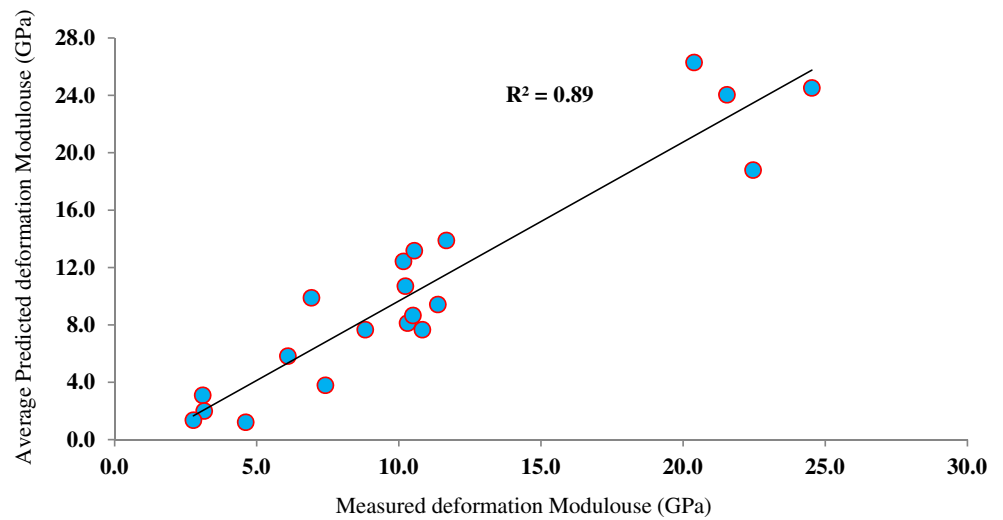
coordinates for a full description. Each element of the (r_{ij}) relation results a pairwise comparison of two data pairs. The strengths of relations (r_{ij}) between output and input parameters can be calculated as follows:

$$r_{ij} = \sum_{k=1}^{m} x_{ik} x_{jk} \Big/ \sqrt{\sum_{k=1}^{m} x_{ik}^2 \sum_{k=1}^{m} x_{jk}^2} \tag{18}$$

Equation (13) reveals that this method is related to dot product for cosine function. Dot product is unity when two vectors are collinear (most similarity) and is zero when the vectors are at the right angles to each other (most dissimilarity). Figure 13 shows the strength values of relations (r_{ij}) between input parameters and

deformation modulus for RBFNN model. According to this figure, the most effective parameters in the deformation modulus are descendingly UCS, weathering, and RQD. Furthermore, bedding/joint inclination to core axis is the least effective parameter in the deformation modulus.

Discussion

The results obtained from statistical analysis of input data have been presented in Fig. 7. The average overburden height of dilatometer test locations is 165 m, based on the above mentioned analyses. According to the results obtained from in situ test (Table 2), there is a confining stress field in the anticline structure. The statistical analyses have shown that the filling thickness is very

Fig. 12 Comparing the measured and average predicted deformation modulus of RBFNN model (BJVC 2009a)
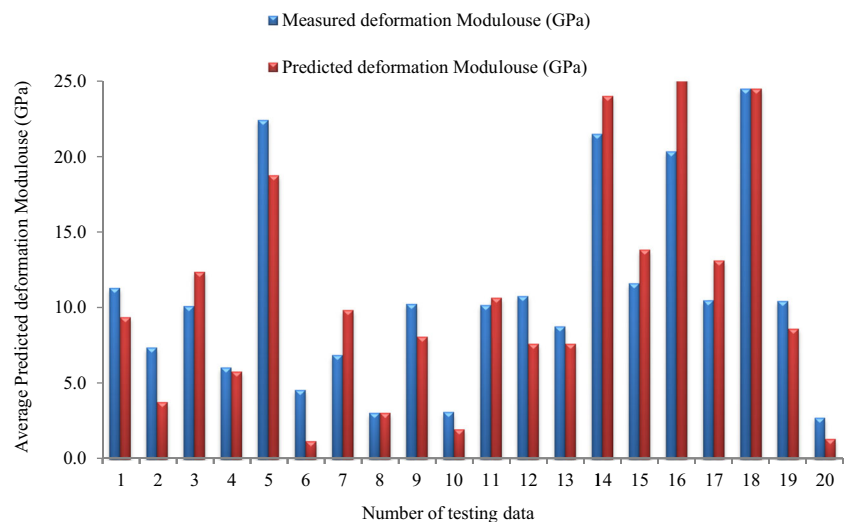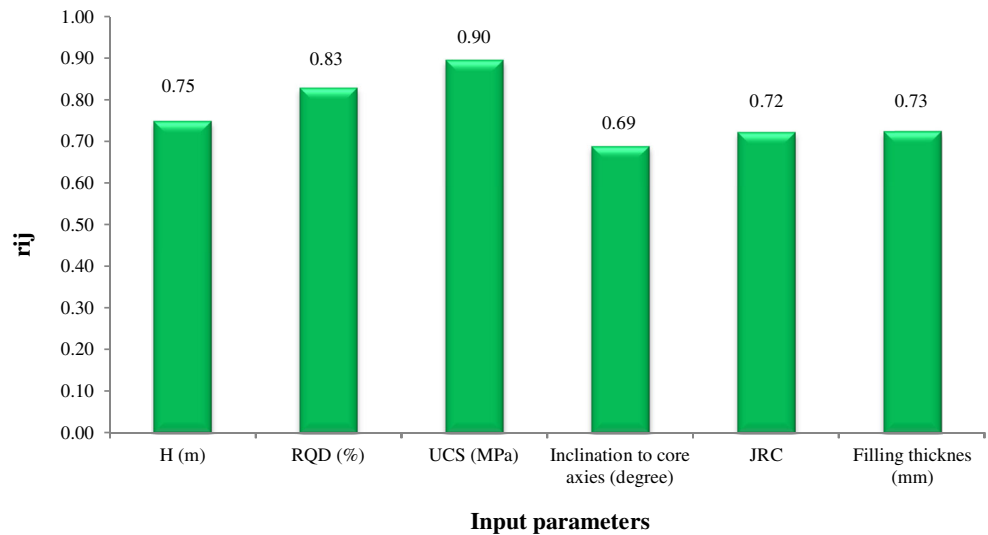
Fig. 13 Strength of relation (r_{ij}) between deformation modulus and input parameters (BJVC 2009a)

low and JRC has average value. It should be noticed that in practice, to avoid jamming the dilatometer apparatus, RQD of test locations is usually high. Accordingly, the average RQD of dilatometer test locations is 90 % (Fig. 7). The results obtained from RBFNN model showed its capability in generalizing complex non-linear relationships between data. The sensitivity analyses showed that UCS and RQD are very influential parameters in deformation behavior of rock mass. As the field stress in dam site completely depends on the tectonic structures, the effect of overburden height is not as important as that of UCS and RQD. Based on the sensitivity analyses, the strengths of relations (r_{ij}) are almost the same between deformation modulus and JRC, and deformation modulus and filling thickness data. Bedding/joint inclination to core axis has the least effect on the deformation modulus at dam site. The horizontal movement of discontinuities is confined by high overburden as well as the presence of horizontal stress field, presented in Table 2. In the high confining stress field, discontinuities may not as much affect the rock mass, comparing to the effect of uniaxial condition. Therefore, with increasing the depth of boreholes and confining stress, bedding/joint inclination to core axis may have lower effect on the deformation modulus of jointed rock mass, in comparison with other parameters.

tests at Bakhtiary dam site. It is observed that the simulation results of RBFNN models are close to the real measured values. Moreover, the threefold cross-validation indicated that the models worked very well with different input data. These findings confirm the comprehensiveness of the model; i.e., the overfitting cannot be a problem. The average performance of proposed model was evaluated by the indices: variance account for (VAF), root-mean-square error (RMSE), mean absolute error (MAE), coefficient of efficiency (CE), and coefficient of correlation (R^2). Optimum average performance of the model was approved by the calculated values of VAF, RMSE, MAE, CE, and R^2 as 83.49%, 2.59, 2.17, 0.88, and 0.89, respectively. The results obtained from this study indicate that the developed RBFNN model can generalize complex non-linear relationships between deformation modulus and other geomechanical properties of rock such as rock quality index, UCS, and JRC. It has been proved that RBFNN model can properly predict rock mass deformation modulus using geomechanical properties of rocks. Finally, sensitivity analyses have been conducted on the model inputs. According to the sensitivity analysis results, performed and obtained from cosine amplitude method (CAM), UCS and RQD are the most effective parameters and bedding/joint inclination to core axis is the least one on the deformation modulus at Bakhtiary dam site.

Conclusion

In this paper, a new RBFNN model has been developed to predict the deformation modulus in geoscience operations based on dilatometer tests. The model is developed on the basis of data sets obtained from in situ dilatometer

References

Barton N (1978) Suggested methods for the quantitative description of discontinuities in rock masses: International Society for Rock Mechanics. Int J Rock Mech Min Sci Geomech Abstr 15(6):319–368

Barton N (2002) some new Q-value correlations to assist in site characterization and tunnel design. Int J Rock Mech Min Sci 39:185–216

Bhushan MV, Sitharam TG (2008) Prediction of elastic modulus of jointed rock mass using artificial neural networks. Geotech Geol Eng 26:443–452

Bieniawski ZT (1974) Geomechanics classification of rock masses and its application in tunneling. In: Proceedings of the third congress of the international society for rock mechanics. Denver: pp 23–32

Bieniawski ZT (1979) The geomechanics classification in rockengineering applications. In: Proceedings of the fourth congress of ISRM, vol 2, Montreux, pp 41–48

Bishop C.M. (1995) Neural Networks for Pattern Recognition. Oxford University Press, New York, pages 482: 165–171

BJVC (2009a) Bakhtiary Dam and HEPP, Engineering geology and rock mechanics report; Report No 4673/4049 Rev 1

BJVC (2009b) Bakhtiary Dam and HEPP, Geological Report, Report No. 4673/4038 Rev 1

Boyd RD (1993) Elastic properties of jointed rock masses with regard to their rock mass rating value. In: Cripps JC et al (eds) The engineering geology of weak rock. Balkema, Rotterdam, pp 329–336

Broomhead DS, Lowe D (1988) Multivariable functional interpolation and adaptive networks. Complex Systems 2:321–355

Cai M, Kaiser PK, Uno H, Tasaka Y, Minami M (2004) Estimation of rock mass deformation modulus and strength of jointed hard rock masses using the GSI system. Int J Rock Mech Min Sci 41:3–19

Ding L, Zhou C (2013) Development of web-based system for safety risk early warning in urban metro construction. Automat Constr 34:45–55

Fahimifar A, Soroush H (2003) Rock mechanics tests, theoretical aspects and standards. Vol. No 1, Published by soil mechanics Laboratory, Tehran

Franklin JA, Dusseault MB (1989) Rock engineering. McGraw-Hill, New York. José M

Ghasemi E, Amini H, Ataei M, Khalokakaei R (2014) Application of artificial intelligenc techniques for predicting the flyrock distance caused by blasting operation. Arab J Geosci 7:193–202

Goodman, Richard E. (1989) Introduction to rock mechanics. Second edition, John Wiley& Sons, New York

Gokceoglu C, Sonmez H, Kayabasi A (2003) Predicting the deformation moduli of rock masses. Int J Rock Mech Min Sci 40:701–710

Grima MA (2000) Neuro-fuzzy modelling in engineering geology. A.A. Balkema, Rotterdam

Guo H, Lin S, Liu J (2006) A radial basis function sliding mode controller for chaotic Lorenz system. Physics Letters A 351:257–261

Habibagahi G, Katebi S (1996) Rockmass classification using fuzzy sets. Iran J Sci Technol Trans B 20(3):273–284

Den Hartog MH, Babuska R, Deketh HJR, Grima MA, Verhoef PNW, Verbruggen HB (1997) Knowledge-based fuzzy model for performance prediction of a rock-cutting trencher. Int J Approx Reason 16(1):43–66

Ham F., Kostanic I. (2001) Principles of Neurocomputing for Science & Engineering. McGraw-Hill, New York

Hoek K (1983) Strength of jointed rock masses. Géotechnique J 23(3):187–223

Hoek E (1994) Strength of rock and rock masses. ISRM New J 2(2):4–16

Hoek E, Brown ET (1997) Practical estimates of rock mass strength. Int J Rock Mech Min Sci 40:701–710

Hoek E, Carranza-Torres C, Corkum B (2002) Hoek–Brown failure criterion-2002 edition. In: Proceedings of 5th North American Rock Mechanics Symposium and Tunneling Association of Canada Conference: NARMS-TAC pp 267–271

Hoek E, Kaiser PK, Bawden WF (1995) Support of underground excavations in hard rock. Balkema, Rotterdam, p 215

Hoek E, Diederichs MS (2006) Empirical estimation of rock mass modulus. Int J Rock Mech Min Sci 43:203–215

Interfels (2002) Dilatometer system, Boart Longyear interfels Gmbh, available at http://www.interfels.com

Jang RJS, Sun CT, Mizutani E (1997) Neuro-fuzzy and soft computing. Prentice-Hall, Upper Saddle River

Karami A, Afiuni-Zadeh S (2012) Sizing of rock fragmentation modeling due to bench blasting using adaptive neuro-fuzzy inference system and radial basis function. Int J Min Sci Technol 22:459–463

Kayabasi A, Gokceoglu C, Ercanoglu M (2003) Estimating the deformation modulus of rock masses: a comparative study. Int J Rock Mech Min Sci 40:55–63

Ladanyi B (1987) Suggested methods for deformability determination using a flexible dilatometer. Int J Rock Mech Min Sci 24(2):123–134

Luo FL, Unbehauen R (1999) Applied neural networks for signal processing. Cambridge University Press, Cambridge

Majdi A, Beiki M (2010) Evolving neural network using a genetic algorithm for predicting the deformation modulus of rock masses. Int J Rock Mech Min Sci 47:246–53

Mitri HS, Edrissi R, Henning J (1994) Finite element modeling of cable-bolted slopes in hard rock ground mines. Presented at the SME annual meeting. Albuquerque, New Mexico, In, pp 94–116

Moosavi M, Yazdanpanah MJ, Doostmohammadi R (2006) Modelling the cyclic swelling pressure of mudrock using artificial neural networks. Eng Geol 87:178–94

Motiei H (1993) Geology of Iran, stratigraphy of Zagros. Geological Survey of Iran publication—Tehran, Iran, In Persian

Narendra BS, Sivapullaiah PV, Suresh SN, Omkar SN (2006) Prediction of unconfined compressive strength of soft grounds using computational intelligence techniques: a comparative study. Comput Geotech 33:196–208

Palmström A, Singh R (2001) The deformation modulus of rock masses—comparisons between in situ tests and indirect esti-mates. Tunnel Undergr Space Technol 16:115–131

Rojas R (1996) Neural networks: a systematic introduction. Springer Verlag, Berlin

Ross T (1995) Fuzzy logic with engineering applications. McGraw-Hill Inc., New York

Serafim JL, Pereira JP (1983) Considerations on the geomechanical classification of Beniawski: experience from case histories. Proceedings of symposium on engineering geology and under-ground openings, Lisbon, In, pp 1133–1144

Sridevi J, Sitharam TG (2003) Characterization of strength and deformation of jointed Rock Mass based on statistical analysis. Int Journal Geomech 3.1:43–54

Sonmez H, Ulusay R (1999) Modifications to the geological strength index (GSI) and their applicability to stability of slopes. Int J Rock Mech Min Sci 36:743–760

Sonmez H, Gokceoglu C, Ulusay R (2004) indirect determination of the modulus of deformation of rock masses based on GSI system. Int J Rock Mech Min Sci 41:849–857 equation. Int J Rock Mech Min Sci 43:224–235

Tan Y, Zhang Z (2011) A RBF neural network approach for fitting creep curve of sandstone. Adv Mater Res Vols 171–172:274–277

Verman M, Singh B, Viladkar MN, Jethwa JL (1997) Effect of tunnel depth on modulus of deformation of rock mass. Rock Mech Rock Eng 30(3):121–127

Yilmaz I, Kaynar O (2011) Multiple Regression, ANN (RBF, MLP) and ANFIS models for prediction of swell potential of clayey soils. Expert Syst Appl 38:5958–5966

Yow JL Jr (1993) Borehole dilatometer testing for rock engineering. Comprehensive rock engineering principles, practice and projects, Vol. 3. Pergamon Press, Oxford, pp 671–682

Zhang L, Einstein HH (2004) Using RQD to estimate the deformation modulus of rock masses. Int J Rock Mech Min Sci 41: 337–341

Zhouquan L, Hongyan Z, Nan J, Yiwei W (2013) Instability identification on large scale underground mined-out area in the metal mine based on the improved FRBFNN. Int J Min Sci Technol 23:821–826